SUPPORTING INFORMATION

Morphing of Amphipathic Helices to Explore the Activity and Selectivity of Membranolytic Antimicrobial Peptides

Alex T. Müller[a], Gernot Posselt[b], Gisela Gabernet[a], Claudia Neuhaus[a], Simon Bachler[c], Markus Blatter[d], Bernhard Pfeiffer[a], Jan A. Hiss[a], Petra S. Dittrich[c], Karl-Heinz Altmann[a], Silja Wessler[b], and Gisbert Schneider[a]*

[a]Department of Chemistry and Applied Biosciences, ETH Zurich, Vladimir-Prelog-Weg 4, 8093 Zürich, Switzerland; [b]Department of Biosciences, Division of Microbiology, Paris Lodron University of Salzburg, Billrothstr. 11, 5020 Salzburg, Austria; [c]Department of Biosystems Science and Engineering, ETH Zurich, Mattenstrasse 26, 4058 Basel, Switzerland; [d]Novartis Institutes for BioMedical Research, Novartis Pharma AG, Novartis Campus, 4002 Basel, Switzerland; *Corresponding author, e-mail: gisbert@ethz.ch

Contents **page**

Video S1, Video S2 (interaction of peptide **6** with a giant POPC vesicle)

Computational activity prediction of designed sequences

All designed sequences were submitted to the CAMP prediction tools to learn about the perception of this current publicly available AMP prediction model[1]. Predictions by all four available machine learning models were obtained and are presented in Table S1.

Extended molecular dynamics simulation methods and results

Table S2 summarizes the parameters that were used during the stages of all molecular dynamics simulations. Figures S2, S3, S4 and S5 show the different conformations obtained in the 100 ns production runs of all peptides.

Circular dichroism spectroscopy at different temperatures

Figure S6 shows the obtained spectra when measuring circular dichroism in 50% TFE at increasing temperatures from 30° to 75° C. The differences in signals observed at 192, 208, and 222 nm when comparing the lowest to the highest temperature were used as a measure of secondary structure stability.

Solution phase nuclear magnetic resonance results

Figure S8 summarizes the Ramachandran plots and sequential restraints obtained by structural calculations from the recorded NMR spectra for peptides Klk14, peptide **6** and peptide **14**.

Table S1. Prediction results obtained through the online AMP prediction tools available on the CAMP website. The higher the values, the more the model interprets the sequence as an AMP. *S. aureus* represents the measured growth-inhibitory activity with ✓ meaning activity at 50 μM or lower.

Peptide	CAMP SVM	CAMP RF	CAMP ANN	CAMP DA	*Staphylococcus aureus*
Klk14	0.70	0.56	1	1.00	✓
Au2.2d2	0.89	0.83	1	0.95	✓
1	0.99	0.98	1	1.00	✓
2	1.00	0.97	1	1.00	✓
3	0.99	0.87	1	1.00	
4	0.99	0.89	1	1.00	
5	0.99	0.89	1	1.00	
6	0.99	0.88	1	1.00	✓
7	0.99	0.86	1	0.99	✓
8	0.95	0.90	1	0.99	✓
9	0.95	0.92	1	0.97	✓
10	0.67	0.83	1	0.93	
11	0.69	0.82	1	0.88	
12	0.32	0.94	1	1.00	
13	0.39	0.91	1	0.99	✓
14	0.44	0.92	1	1.00	✓
15	0.50	0.95	1	1.00	✓
16	0.55	0.95	1	1.00	✓
17	0.43	0.56	1	1.00	✓
18	0.53	0.58	1	1.00	

Table S2. Parameters used for the different stages of all molecular dynamics simulations in 50% 2,2,2-trifluoroethanol + water.

	Minimization	NVT Equilibration	NPT Equilibration	Production Run
No. of steps	Ftol = 1000.0 kJ/mol/nm	25000 (50ps)	25000 (50ps)	500000 (1ns)
Propagation	Steepest Decent	Leap-Frog Verlet	Leap-Frog Verlet	Leap-Frog Verlet
Ensemble	-	NVT (mod. Berendsen thermostat)	NPT (Parrinello-Rahman)	NPT (Parrinello-Rahman)
tau p	-	-	2	2
tau T	-	0.1	0.1	0.1
Peptide constratnts	-	all bonds	all bonds	all bonds
Constraint algorithm	-	LINCS	LINCS	LINCS
Cutoff-scheme	Verlet	Verlet	Verlet	Verlet
Coulomb type	PME	PME; order: 4	PME; order: 4	PME; order: 4
Short range vdW cutoff	1nm	1nm	1nm	1nm
Short range electrostatic cutoff	1nm	1nm	1nm	1nm
Fourier spacing	-	0.16nm	0.16nm	0.16nm
Reference temperature	-	300 K	300 K	300 K
Reference pressure	-	-	1 bar	1 bar
Periodic boundary conditions	3D PBC	3D PBC	3D PBC	3D PBC

Table S3. Measured and modeled helical secondary structure content in % helicity. CD: circular dichroism spectroscopy; MD: average helical content over a 100 ns molecular dynamics simulation; W: water; T: 50% 2,2,2-trifluoroethanol (TFE) in water; Ind: helical induction in presence of TFE compared to water (value in TFE divided by value in water). ∗ Active peptides against *Staphylococcus aureus* SH1000 at concentrations of 50 µM or less.

Peptide	CD_W	CD_T	CD_{Ind}	MD_W	MD_T	MD_{Ind}
Au2.2d2*	28	71	2	12	27	2
Klk 14*	25	58	2	24	68	2
1*	15	55	3	11	65	5
2*	15	57	3	27	70	2
3	28	66	2	23	58	2
4	29	66	2	28	71	2
5	25	59	2	15	63	4
6*	23	68	2	25	56	2
7*	25	63	2	5	44	8
8*	20	57	2	12	31	2
9*	15	64	4	1	24	16
10	24	61	2	3	50	14
11	9	60	6	28	41	1
12	9	54	5	13	26	2
13*	11	53	4	1	27	14
14*	9	53	5	4	44	10
15*	9	53	5	15	43	2
16*	19	56	2	22	63	2
17*	15	58	3	13	54	3
18	20	58	2	5	66	12

Table S4. Analytics data. MW: calculated molecular weight [g/mol], tR: measured retention time, m/z: main detected masses in the chromatogram.

Peptide	MW	t_R [min]	m/z
Klk14	1691.36	9.3	564.5, 422.6
Au2.2d2	1414.76	12.5	708.1, 472.4
1	1620.23	10.5	810.7, 540.8
2	1654.25	10.4	827.8, 552.2
3	1641.16	12.3	821.1, 547.8
4	1641.16	12.2	821.1, 547.8
5	1627.14	12.1	814.2, 543.2
6	1613.11	11.9	807.2, 538.5
7	1599.08	11.2	800.2, 533.8
8	1527.96	12.1	764.6, 510.1
9	1485.88	10.6	827.8, 552.2
10	1485.88	10.6	743.6, 496.1
11	1451.86	10.9	1452.3, 484.8
12	1464.95	7.9	733.2, 489.1
13	1464.95	8.1	733.2, 489.1
14	1478.98	8.7	740.2, 493.8
15	1493.00	9.2	747.2, 498.5
16	1507.03	9.7	754.2, 503.1
17	1578.15	9.4	526.9, 395.4
18	1620.23	9.9	810.8, 540.9

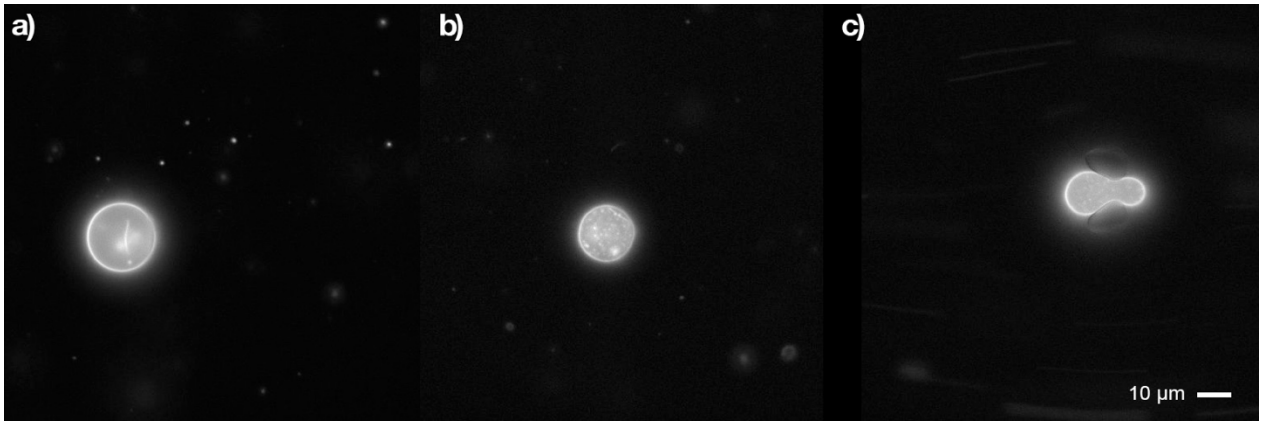

Figure S1. Images of giant POPC vesicles with membrane-incorporated DiD dye, floating in the microfluidic chip chamber and later used for rupturing studies (see Video S1 and S2). **a)** Giant vesicle **b)** Partially multilamellar giant vesicle **c)** Vesicle trapping under continuous flow (from left to right).

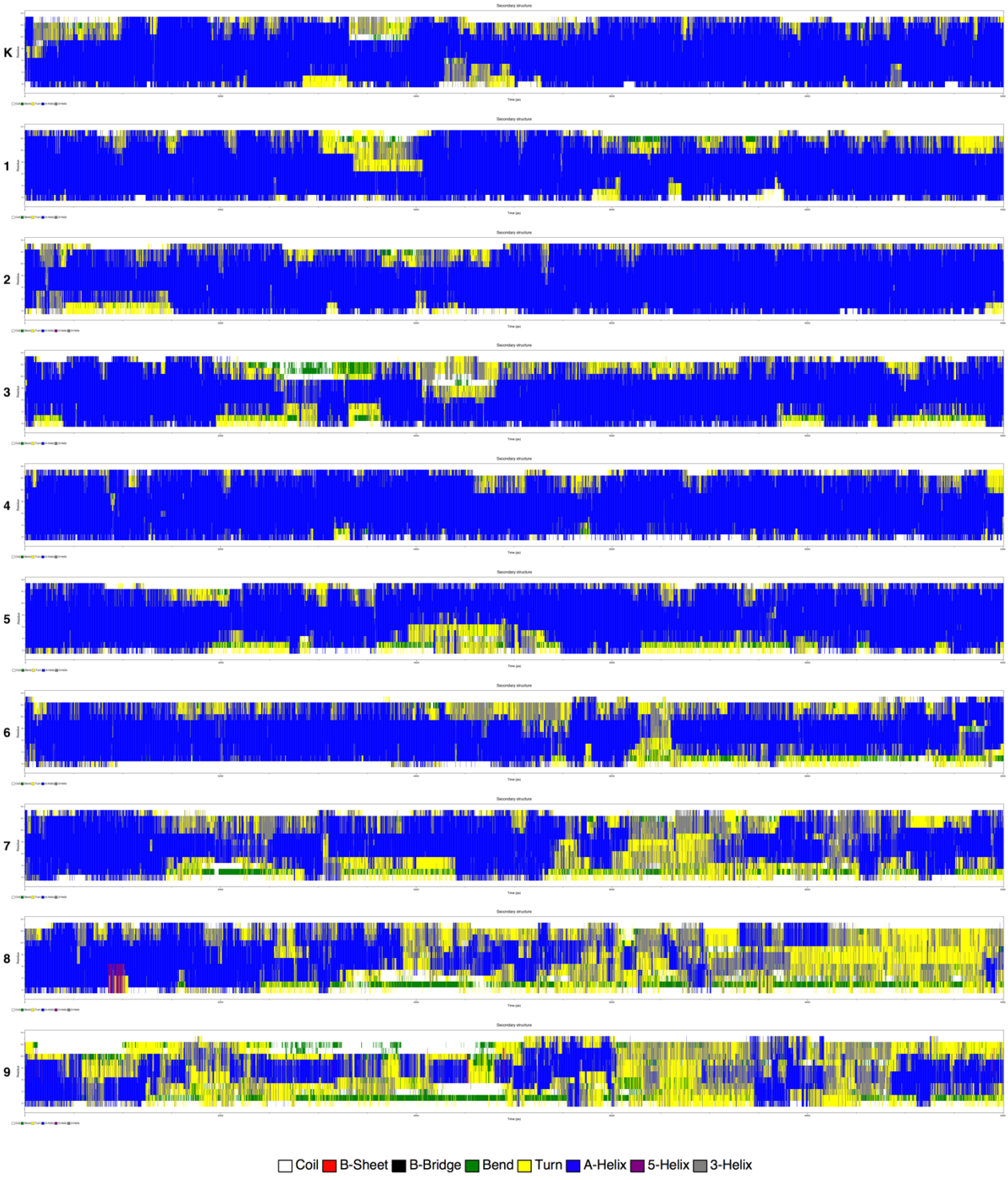

Figure S2. Secondary structure over 100 ns molecular dynamics simulation trajectory of peptides Klk 14 (K) and 1-9 (in this order) simulated **in 50% TFE**. The x-axis shows the simulation time and the y-axis the peptide sequence from N-terminus (bottom) to C-terminus (top).

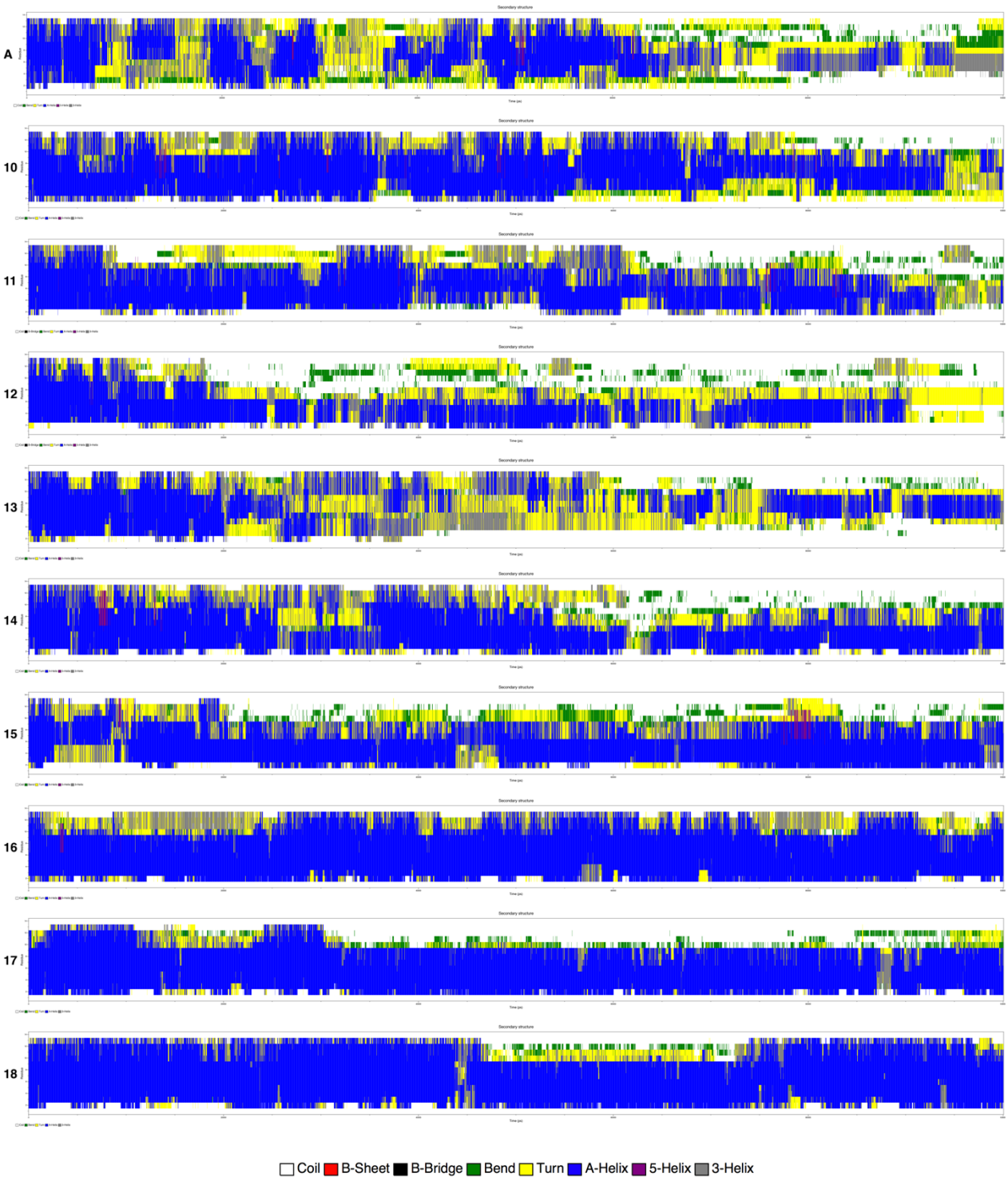

Figure S3. Secondary structure over 100 ns molecular dynamics simulation trajectory of peptides Au2.2d2 (A) and 10-18 (in this order) simulated **in 50% TFE**. The x-axis shows the simulation time and the y-axis the peptide sequence from N-terminus (bottom) to C-terminus (top).

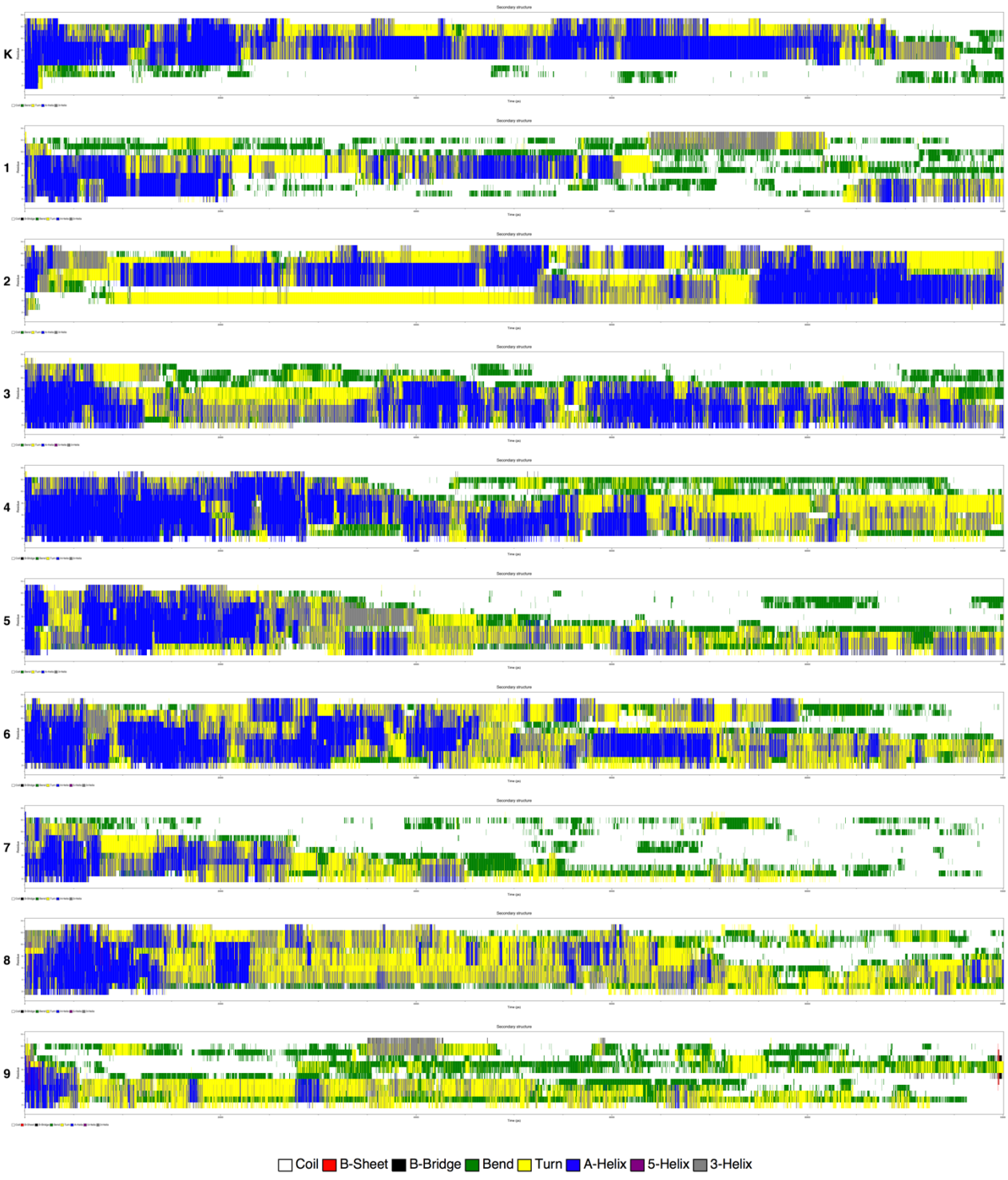

Figure S4. Secondary structure over 100 ns molecular dynamics simulation trajectory of peptides Klk 14 (K) and 1-9 (in this order) simulated **in water**. The x-axis shows the simulation time and the y-axis the peptide sequence from N-terminus (bottom) to C-terminus (top).

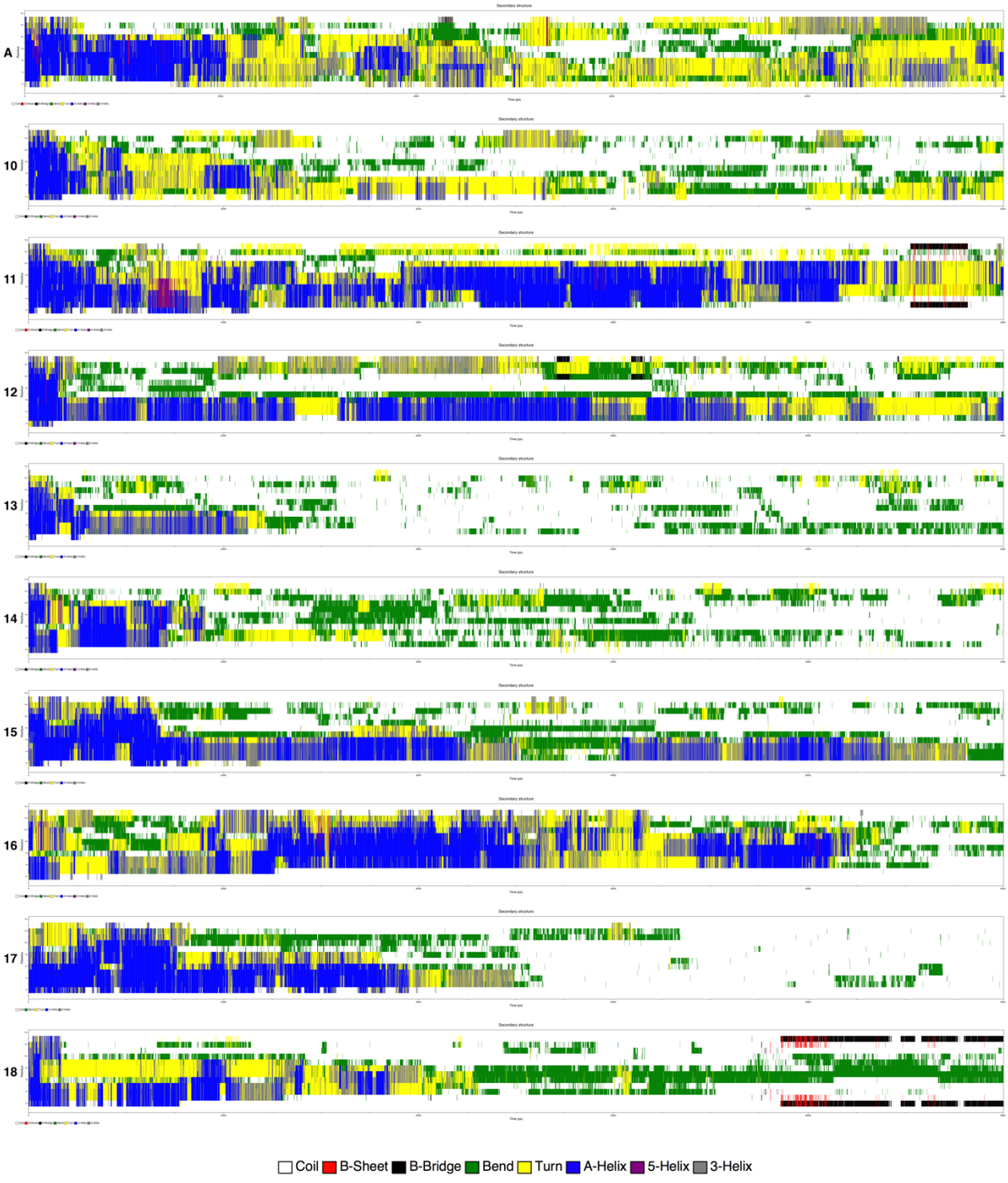

Figure S5. Secondary structure over 100 ns molecular dynamics simulation trajectory of peptides Au2.2d2 (A) and 10-18 (in this order) simulated **in water**. The x-axis shows the simulation time and the y-axis the peptide sequence from N-terminus (bottom) to C-terminus (top).

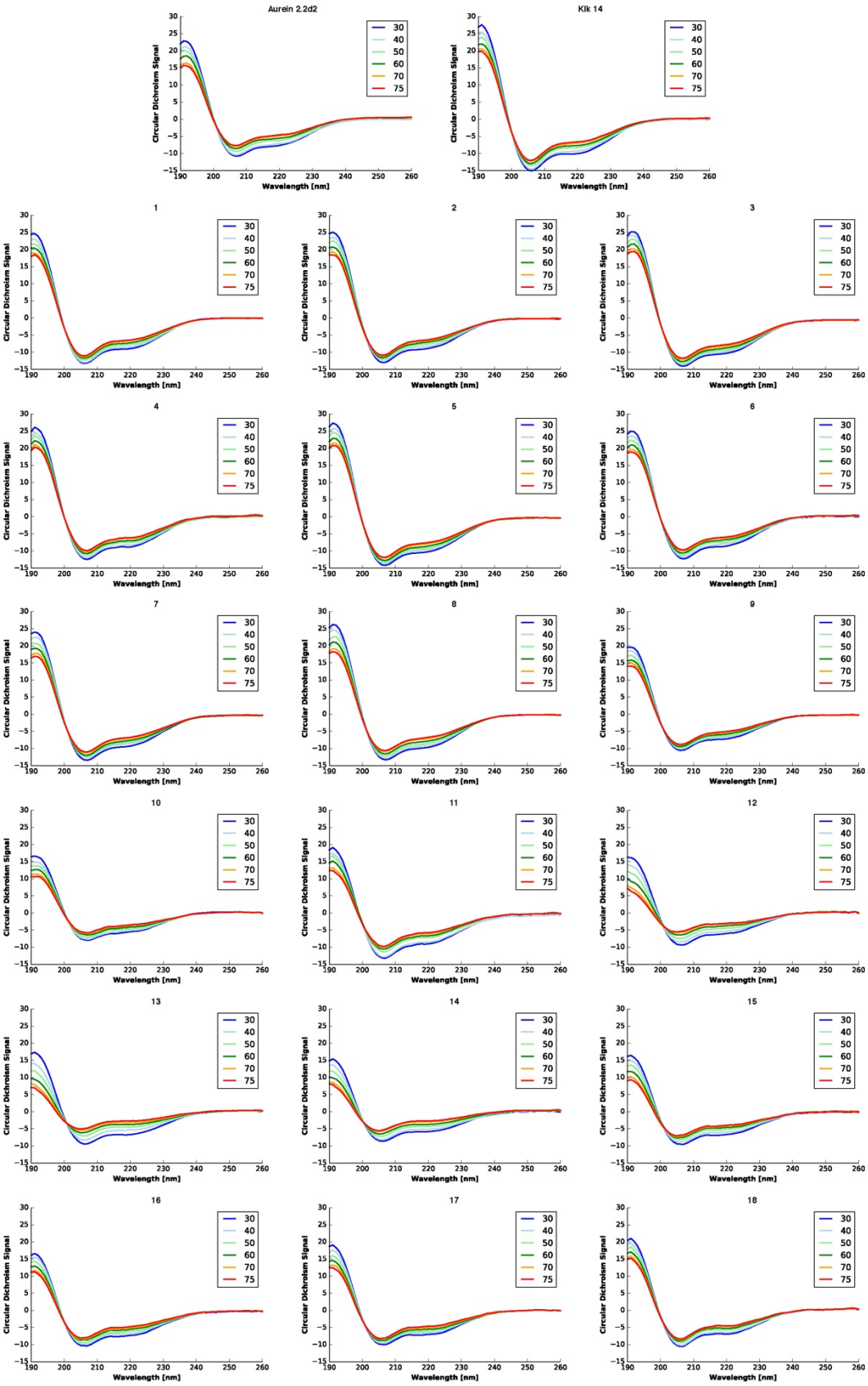

Figure S6. Circular dichroism spectra of all peptides recorded at six different temperatures in 50% 2,2,2-trifluoroethanol+water.

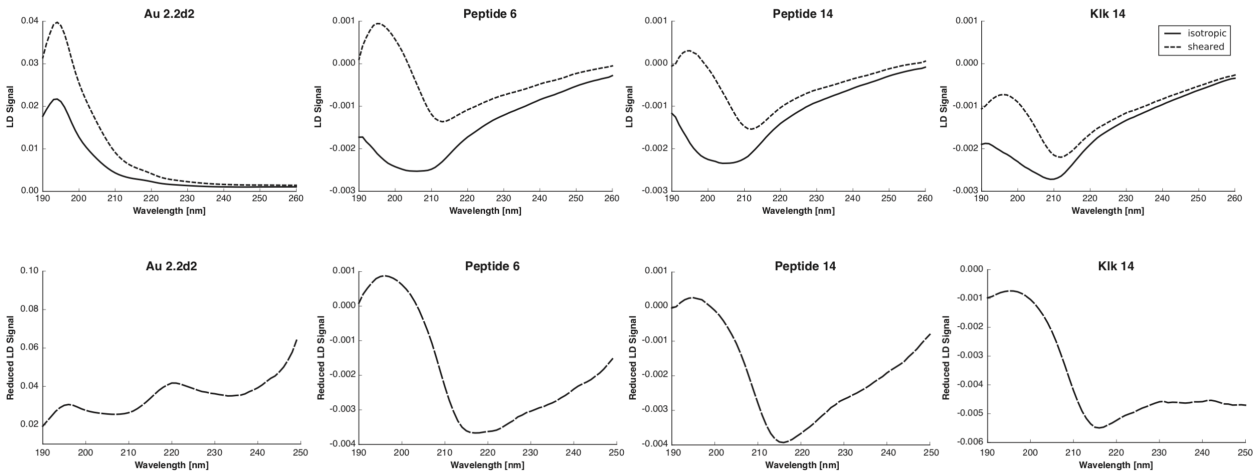

Figure S7. Linear dichroism spectra of four selected peptides recorded in cationic liposomes (N=2). Au2.2d2 and Klk14 represent the endpoints of the morphing run, 6 and 14 represent two intermediate peptides. 6 was found to be the most active peptide on *Staphylococcus aureus* SH1000, whereas 14 was the most broadly active and selective peptide. One can observe profound differences in the LD spectra when comparing isotropic (non-spinning) to sheared conditions, as well as when comparing spectra inter-peptide wise. **top**: Linear dichroism signals of sheared and isotropic (non-spinning) conditions. **bottom**: Reduced linear dichroism signals where LD spectra were divided by the corresponding absorbance spectra at isotropic conditions. Spectra were cut at 250 nm because of artifacts caused by the division.

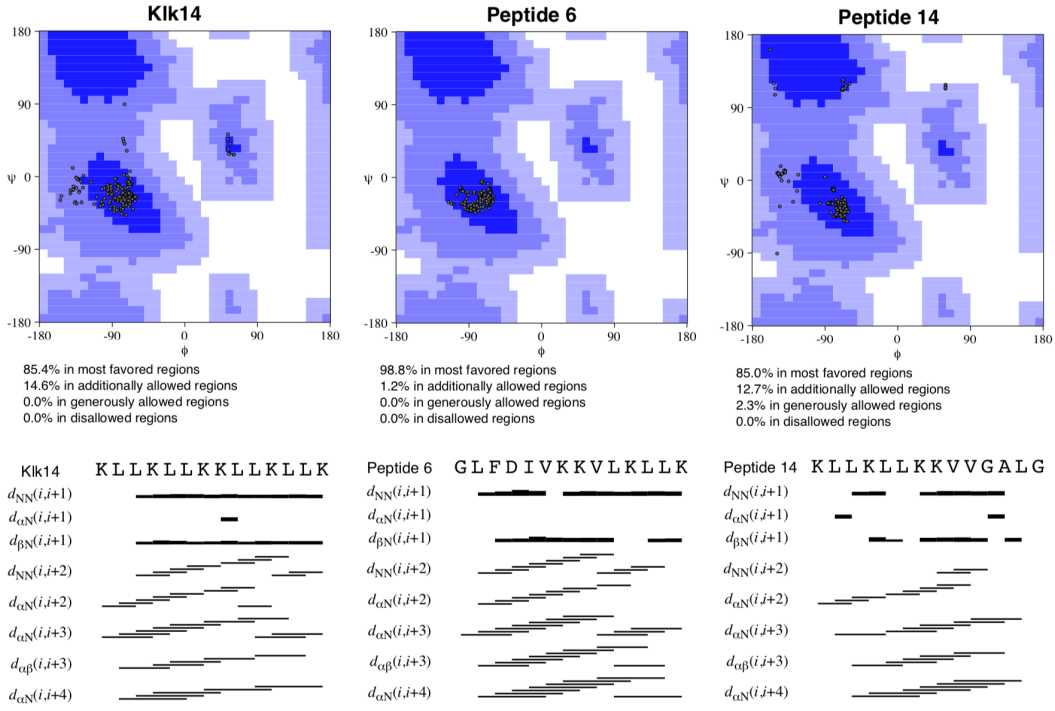

Figure S8. Ramachandran plots (**top**) and sequence restraints (**bottom**) for the recorded NMR spectra.

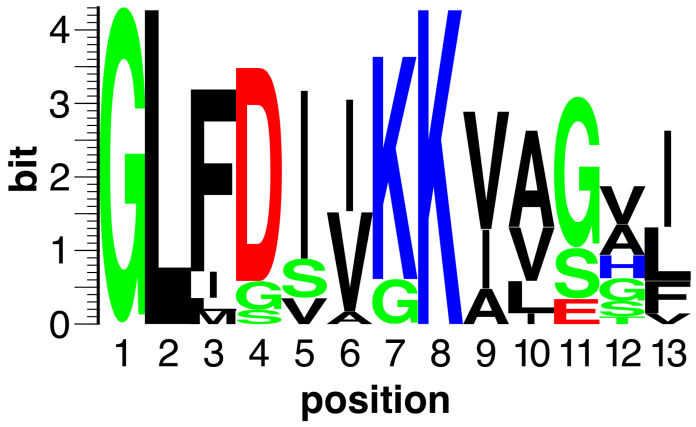

Figure S9. Sequence logo of Aurein and Citropin AMPs generated with the RTH web tool (URL: https://rth.dk/resources/plogo/)[1,2], assuming equal a priori amino acid probabilities. The first 13 amino acids of the sequences were used, as this is the length of the shortest peptide in the family. The y axis shows the amount of information contained at each sequence position.

Table S5. Sequence positional entropy values calculated with the RTH web tool (*https://rth.dk/resources/plogo/*)[1,2], assuming equal a priori amino acid probabilities.

Sequence Position	1	2	3	4	5	6	7	8	9	10	11	12	13
Shannon Information	4.322	4.322	3.224	3.519	3.2	3.07	3.672	4.322	2.907	2.646	3.098	1.88	2.646

Table S6. Aurein and Citropin sequences used to generate the alignment, sequence logo and Shannon information values in Figure S9 and Table S5.

Name	**Sequence**	**Name**	**Sequence**
Aurein 1.1	GLFDIIKKIAESI	Citropin 1.2	GLFDIIKKVASVVGGL
Aurein 1.2	GLFDIIKKIAESF	Citropin 1.3	GLFDIIKKVASVIGGL
Aurein 2.1	GLLDIVKKVVGAFGSL	Citropin 2.1	GLIGSIGKALGGLLVDVLKPKL
Aurein 2.2	GLFDIVKKVVGALGSL	Citropin 2.1.3	GLIGSIGKALGGLLVDVLKPKLQAAS
Aurein 2.3	GLFDIVKKVVGAIGSL	Citropin 1.1.3	GLFDVIKKVASVIGLASP
Aurein 2.4	GLFDIVKKVVGTLAGL		
Aurein 2.5	GLFDIVKKVVGAFGSL		
Aurein 2.6	GLFDIAKKVIGVIGSL		
Aurein 3.1	GLFDIVKKIAGHIAGSI		
Aurein 3.2	GLFDIVKKIAGHIASSI		
Aurein 3.3	GLFDIVKKIAGHIVSSI		
Aurein 5.2	GLMSSIGKALGGLIVDVLKPKTPAS		

Table S7. Flexibility scale[4] used to calculate peptide flexibility values in this work.

Amino Acid	Flexibility Value
M	0
F	0.042
W	0.042
H	0.083
C	0.208
A	0.25
L	0.292
V	0.375
Y	0.5
T	0.583
I	0.667
N	0.667
K	0.708
Q	0.792
E	0.833
D	0.875
P	0.875
S	0.875
R	0.958
G	1

Figure S10. Helical wheel plots with hydrophobic moments for all peptides (modlAMP Eisenberg scale, www.modlamp.org).

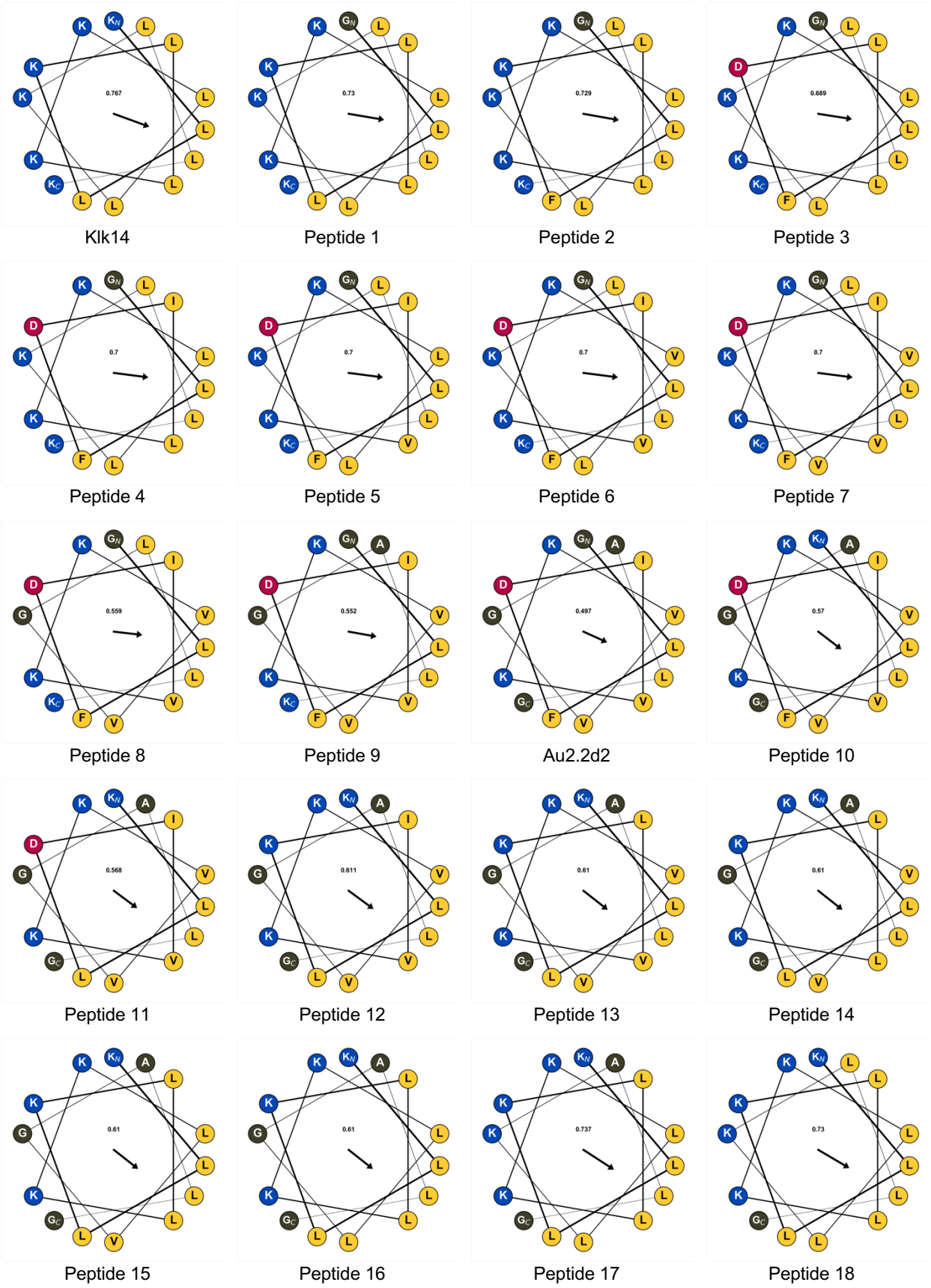

CO-ADD Antimicrobial and Antifungal Screening

Assays were performed by the Community for Open Antimicrobial Drug Discovery (CO-ADD, www.co-add.org), The University of Queensland, 306 Carmody Road, St Lucia QLD 4072, Australia.

Antimicrobial and antifungal activities were determined in two steps. Primary antimicrobial screening was performed by whole cell growth inhibition assays, using the sample compounds at a single concentration, in duplicate (*n*=2). The inhibition of growth was measured against five bacteria (ATCC strain ID): *Escherichia coli* (ATCC 25922), *Klebsiella pneumoniae* (ATCC 700603)*, Acinetobacter baumannii* (ATCC 19606)*, Pseudomonas aeruginosa* (ATCC 27853), *Staphylococcus aureus* (ATCC 43300), and two fungi: *Candida albicans* (ATCC 90028), *Cryptococcus neoformans* (ATCC 208821).

Primary screening conditions:

Test concentration: 32µg/ml or 20 µM (≤1% DMSO), QC: duplicate (*n*=2), Control MIC: Pass, Plates: 384-wells with non-binding surface, Media: bacterial: cation-adjusted Mueller Hinton broth, fungi: yeast nitrogen base, Read-Out: bacteria OD_{600}, *C. albicans* OD_{530}, *C. neoformans* resazurin $OD_{600\text{-}570}$.

To confirm the inhibitory activity, the hit compound/s were be re-tested against the strains in a dose response assay to determine the minimum inhibitory concentration (MIC) of the compounds. To further evaluate the antimicrobial potential of the compounds they were be assayed against a mammalian cell line to determine general cell toxicity. Samples were provided by the collaborator and stored frozen at -20 °C. Samples were prepared in DMSO and water to a final testing concentration of 32 µg/mL or 20 µM (unless otherwise indicated in the data sheet), in 384-well, non-binding surface plate (NBS) for each bacterial/fungal strain, and in duplicate (*n*=2), and keeping the final DMSO concentration to a maximum of 1% DMSO. All the sample-preparation where done using liquid handling robots.

Antimicrobial Assay

All bacteria were cultured in Cation-adjusted Mueller Hinton broth (CAMHB) at 37 °C overnight. A sample of each culture was then diluted 40-fold in fresh broth and incubated at 37 °C for 1.5–3 h. The resultant mid-log phase cultures were diluted (CFU/mL measured by OD_{600}), then added to each well of the compound containing plates, giving a cell density of 5×10^5 CFU/mL and a total volume of 50 µL. All the plates were covered and incubated at 37 °C for 18 h without shaking.

Inhibition of bacterial growth was determined measuring absorbance at 600 nm (OD_{600}), using a Tecan M1000 Pro monochromator plate reader. The percentage of growth inhibition was calculated for each well, using the negative control (media only) and positive control (bacteria without inhibitors) on the same plate as references. The significance of the inhibition values was determined by modified *z*-scores, calculated using the median and MAD of the samples (no controls) on the same plate. Samples with inhibition value above 80% and *z*-score above 2.5 for either replicate (*n*=2 on different plates) were classed as actives. Samples with inhibition values between 50–80% and z-score above 2.5 for either replicate (*n*=2 on different plates) were classed as partial actives. Samples with inhibition values between 50–80% and *z*-score above 2.5 for either replicate (*n*=2 on different plates) were classed as partial actives.

Antifungal Assay

Fungi strains were cultured for 3 days on Yeast Extract-Peptone Dextrose (YPD) agar at 30 °C. A yeast suspension of 1×10^6 to 5×10^6 CFU/mL (as determined by OD_{530}) was prepared from five colonies. The suspension was subsequently diluted and added to each well of the compound-containing plates giving a

final cell density of fungi suspension of 2.5×10^3 CFU/mL and a total volume of 50 µL. All plates were covered and incubated at 35 °C for 24 h without shaking.

Growth inhibition of *C. albicans* was determined measuring absorbance at 530 nm (OD_{530}), while the growth inhibition of *C. neoformans* was determined measuring the difference in absorbance between 600 and 570 nm ($OD_{600-570}$), after the addition of resazurin (0.001% final concentration) and incubation at 35 °C for additional 2 h. The absorbance was measured using a Biotek Synergy HTX plate reader. The percentage of growth inhibition was calculated for each well, using the negative control (media only) and positive control (fungi without inhibitors) on the same plate. The significance of the inhibition values was determined by modified Z-scores, calculated using the median and MAD of the samples (no controls) on the same plate. Samples with inhibition value above 80% and *z*-score above 2.5 for either replicate (*n*=2 on different plates) were classed as actives. Samples with inhibition values between 50–80% and *z*-score above 2.5 for either replicate (*n*=2 on different plates) were classed as partial actives.

Quality control

Colistin and Vancomycin were used as positive bacterial inhibitor standards for Gram- negative and Gram-positive bacteria, respectively. Fluconazole was used as a positive fungal inhibitor standard for *C. albicans and C. neoformans.* The antibiotics were provided in 4 concentrations, with 2 above and 2 below its MIC value, and plated into the first 8 wells of column 23 of the 384-well NBS plates. The quality control (QC) of the assays was determined by the antimicrobial controls and the Z'-factor (using positive and negative controls). Each plate was deemed to fulfil the quality criteria (pass QC) if the *z'*-factor was above 0.4, and the antimicrobial standards showed full range of activity, with full growth inhibition at their highest concentration, and no growth inhibition at their lowest concentration. All antibiotic controls displayed inhibitory values within the expected range.

References

1. Waghu, F. H., Barai, R. S., Gurung, P., Idicula-Thomas S. (2016) CAMPR3: a database on sequences, structures and signatures of antimicrobial peptides. *Nucleic Acids Res. 44*, D1094–D1097.
2. Gorodkin, J., Heyer, L. J., Brunak, S., Stormo G. D. (1997) Displaying the information contents of structural RNA alignments: the structure logos. *Comput. Appl. Biosci. 13*, 583–586.
3. Schneider, T. D., Stephens, R. M. (1990) Sequence logos: a new way to display consensus sequences. *Nucleic Acids Res. 18*, 6097–6100.
4. Bhaskaran R. Ponnuswamy P. K. (1988) Positional flexibilities of amino acid residues in globular proteins. *Int. J. Pept. Protein Res*., 32, 241–255.